ARTICLE

Duonco: A Dual Nanovesicle Drug Delivery System for Breast Cancer

Ananya Aravind, Devashish Kalmegh, Harshini Sivanganam, Gopal K., Ira Zibbu, Jyothi S., Kapavarapu Pratham, Kavya Sunil, Merina Tony, Nikhil Nawaz, Parth Ankam, Pranav Thapron, Riya Shende, Siddharth Kurne, Sneha P. R.

Indian Institute of Science Education and Research, Thiruvananthapuram, India
Contact for correspondence: IISER TVM, Email: igem@iisertvm.ac.in.

Abstract

Contemporary cancer drug therapies have poor specificity, and developing drugs that preferentially affect tumour cells represents an open challenge in the field. Single cancer marker targeting strategies like monoclonal antibodies have advantages over conventional drugs but lack additional checkpoints for specificity. Here we describe a new nanovesicle-based drug delivery system for breast cancer that utilises two cancer biomarkers to target cancer cells. This system is analogous to an AND gate, where the drug is only activated in cells that overexpress both markers. Two types of bioengineered *E. coli* outer membrane vesicles (OMVs) are generated, each targeting one of the two HER2+ breast cancer cell-surface markers: HER2 and CX3CR1. Anti-HER2 OMVs are loaded with a prodrug and anti-CX3CR1 OMVs are loaded with an enzyme. When both OMVs are internalised into a cancer cell overexpressing both markers, drug activation occurs, followed by cell death. In cells with basal expression of the markers, single OMV or no OMV internalisation is anticipated, the drug remains inactivated in the absence of the prodrug, resulting in minimal effect. We propose that such an adaptable dual OMV system has great potential for cell-specific targeting of a variety of cancer cells, as well as use in personalised medicine.

Keywords: breast cancer, drug delivery, bioengineering

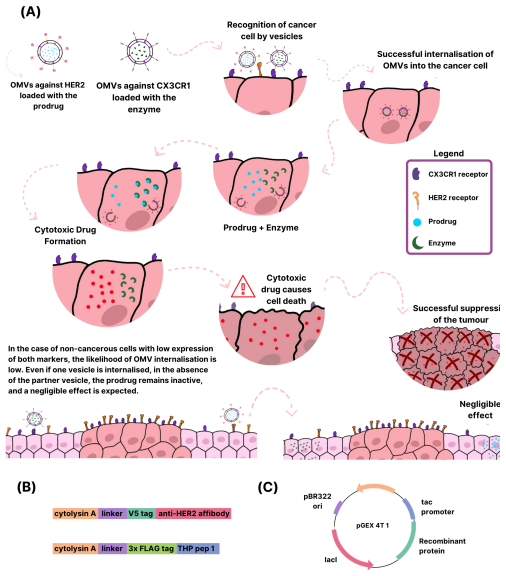

Figure 1. Fig 1: (A) An overview of the mechanism (B) Design of recombinant affinity proteins (C) pGEX-4T1 backbone

Background

Cancer research is an ever-evolving field. Extensive efforts by countless researchers in the past have opened up diverse options for therapeutic intervention. However, a fundamental issue in drug therapy for cancer is that current chemotherapeutic drugs have poor specificity and indiscriminately affect cancerous and non-cancerous cells [1]. Developing drugs that preferentially target tumour cells represents a grand challenge in cancer therapy research that is of significant interest to biomedical researchers, patients, medical practitioners, and pharmaceutical companies. Although we are addressing the broader problem of improving the specificity of chemotherapy, we chose breast cancer as our model due to its prevalence in India, and in our local community in Thiruvananthapuram.

In 2020, there were 2.3 million new cases of breast cancer and 685,000 deaths globally. Currently, in India, breast cancer has the highest gross incidence and mortality among all cancers. Projections from the WHO Global Cancer Observatory suggest that by 2040, there could be 3.9 million new cases and 1.04 million deaths worldwide [2]. Socio-economic inequalities compound the issue in India by limiting access to life-saving diagnostics and treatment. Over 40 percent of households across India resort to distress funding to cover the cost of cancer treatment [3]. As cases continue to rise, the next few years represent a crucial moment to change how we think about breast cancer therapy.

Cancer cells differentially overexpress specific cell surface markers. Targeted therapies capitalise on this property of cancer cells to preferentially attack cancerous cells. However many non-cancerous cells have basal expression of the cell surface marker and are thereby affected by the drug. Monoclonal antibodies against HER2 such as trastuzumab and pertuzumab are more effective than traditional chemotherapies, but are associated with off-site toxicity and the development of resistant cancers [4] [5]. We wanted to build a more robust system by utilising not one, but two targets. The functioning of this system is analogous to an AND gate: the drug is activated only in cells overexpressing both markers, and any cell expressing one or none of the markers remains largely unaffected. This second marker would therefore serve as an additional checkpoint.

Project Design

The ideal target cancer biomarkers for Duonco are those that have shown to be overexpressed in breast cancer, and have an accessible extracellular domain. Among the different molecular subtypes of breast cancer, we chose HER2+ breast cancer due to the availability of such markers. Other subtypes are characterised by nuclear-localised markers (such as estrogen or progesterone) or altogether lack defined markers (as with triple-negative breast cancer), and are not an ideal model system to test Duonco [6]. Among the cell surface markers associated with HER2+ breast cancer, we chose HER2 and CX3CR1.

The Human Epidermal Growth Factor Receptor 2 (HER2), also known as ErbB2, is a protein with an essential role in cell differentiation and growth. Overexpression of HER2 is associated with malignancy in cells, and occurs in approximately 15-30 percent of breast cancers. It is strongly associated with increased disease recurrence and a poor prognosis [7].

CX3C motif chemokine receptor 1 (CX3CR1 is a G protein-coupled receptor. It is responsible for modulating cell activity towards survival, migration and proliferation. CX3CR1 has been shown to be important in driving metastasis in breast cancer [8]. Research on using CX3CR1 as a target is not as abundant as for HER2, but some studies have indicated that it may be a viable target.

We chose Bacterial Outer Membrane Vesicles (OMVs) to be our drug carrier of choice. OMVs are non-replicating nanovesicles that are produced by the blebbing of the outer membrane of gram-negative bacteria with mean diameter between 20 to 200 nm [9]. There are several advantages to using OMVs for targeted drug delivery. OMVs can easily be decorated with heterologous proteins and can carry diverse payloads. They protect their contents from the external environment and dilution [10]. In addition, they also have intrinsic immunostimulatory properties, thus synergistically helping the body's innate immune system in the targeting of cancer cells [11].

We intended to express affinity proteins on the surface of the OMVs to direct the vesicles towards the tumour cells. We chose an anti-HER2 affibody ZHER2:342 to be expressed on the surface of the OMVs to create Affi-OMVs targeting HER2 [12]. ZHER2:342 is an engineered protein that binds to the extracellular domain of HER2 with remarkable affinity to HER2 (Kd = 22 pM) [12]. We chose Tumour Homing Peptide 1 (THP Pep-1) to be expressed on the surface of another set of OMVs to generate THP-OMVs targeting CX3CR1 [13]. THPs are engineered oligopeptides (< 30 residues) that selectively bind to specific markers on tumour cells. Their small size, low immunogenicity, high specificity and versatility makes them ideal for a variety of purposes [14]. Affinity proteins such as affibodies and peptides can be expressed on the surface of OMVs by genetically fusing them to a bacterial protein that naturally translocates to the outer membrane, and concomitantly, OMVs. We used Cytolysin A (ClyA) for this purpose [15]. Our generated recombinant proteins have ClyA at the N terminus, followed by a flexible serine-glycine (SG), an epitope tag for detection and the affinity protein at the C terminus (Fig 1B).

The engineered OMVs would be integrated with a prodrug-enzyme system in order to limit the offsite targeting effect observed. The prodrug-enzyme system consists of an inactive prodrug that is activated by its cognate enzyme. This activated form of the drug would then produce a therapeutic effect (cancer cell death). The prodrug-enzyme system enables a more precise regulation of the therapeutic effect by controlling when and where the prodrug and enzyme interact [16]. For this project, we chose cytosine deaminase. Cytosine deaminase converts 5-fluorocytosine (5FC) to 5-fluorouracil (5FU). 5FU traverses into the neighbouring cells. It exerts its anticancer action through inhibition of thymidylate synthase and incorporation of its metabolites RNA and DNA. If injected at the core of the tumour, even a small amount of the activated drug should be enough to cause a significant decrease in the size of the tumour [17].

These recombinant proteins are expressed separately in two populations of *E.coli*, where they translocate to the outer membrane of the bacteria. One population produces Affi-OMVs against HER2 and THP-OMVs against CX3CR1. Affi-OMVs are loaded with the prodrug and THP-OMVs with the enzyme respectively. We hypothesise that when Affi-OMVs and THP-OMVs are administered and encounter a cancer cell expressing HER2 and CX3CR1, they are simultaneously internalised, and release their contents. The prodrug is converted to its active drug form by the enzyme and exerts its therapeutic effect. In the case of a non-cancerous cell having basal expression of one or both of these receptors, the probability of simultaneous internationalisation is low. Even if one type of OMV is internalised, in the absence of its partner, the drug remains inactivated and a negligible effect is expected (Fig 1A).

With this project, we hope to develop a prototype for a versatile system that furthers the specificity of drug therapy in cancer. The dual marker targeting approach is an improvement over current single marker targeted therapies. Although it is being developed for breast cancer, Duonco can be modified for use in other types of cancers by varying the affinity proteins. It also has applications in personalised medicine where the affinity proteins can be tailored to the specific biomarker profile of the patient.

Results

Selecting a hypervesiculating E. coli strain for OMV production

Standard laboratory strains of *E. coli* have minimal production of OMVs in culture. We obtained four *E. coli* K12 single gene knockout strains (tolA::Kan, tolR::Kan, nlp::Kan, degP::Kan) from the Keio collection that were previously re-

ported to have improved yield of OMVs over the parental K12 strain [18][19][20]. We compared growth curves and the final OD600 of the strains to gain a rough estimate of the fitness cost of the gene knockouts. degP showed delayed growth kinetics and the lowest final OD600 (Fig 2A). Additionally, tolR is reported to produce more OMVs than tolA, and we excluded both strains from the remainder of the project.

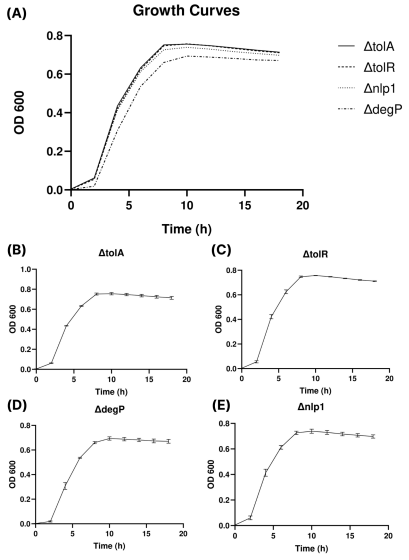

Figure 2. (A) Comparative analysis of growth curves of four hypervesiculating *E. coli* strains. Individual growth curves of (B) tolA (C) tolR (D) degP and (E) nlp1. Error bars indicate mean ± standard error of the mean of three biological replicates, each having two technical replicates.

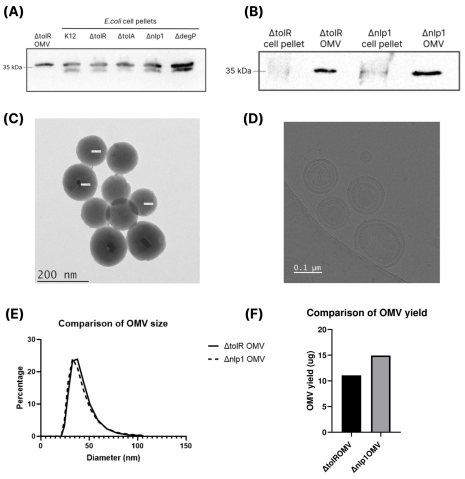

Figure 3. (A) Anti-OmpA Western blot of OMVs isolated from tolR, and bacterial pellets of parental strain *E.coli* K 12 and hypervesiculating strains tolA, tolR, nlp1 and degP. Bands were detected at the expected size of 37 kDa. An additional lower molecular weight band was noted in the bacterial pellets, that was absent in the OMV fraction. (B) Anti-OmpA Western blot of OMV fractions from *E. coli* tolR and *E. coli* nlp1. Equal volumes were loaded for the OMV samples. Cell pellets of both strains were also analysed, but the presence of excess sample in these lanes hindered the proper resolution of proteins during electrophoresis, causing a hazy and diffused appearance (C) Transmission electron microscope image of OMVs isolated from *E. coli* tolR. (D) Cryogenic transmission electron microscope images of OMVs from *E. coli* tolR. (E) Comparison of the size distribution of OMVs from *E. coli* tolR and *E. coli* nlp1. The X axis indicates diameter (in nm) and the Y axis indicates the percentage. There is a strong correspondence between the two distributions. Average diameter of *E. coli* tolR OMVs = 40 nm, average diameter of *E. coli* nlp1 OMVs = 39 nm (F) Comparative analysis of the OMV yield from two *E .coli* strains. OMV yield is measured as total protein in the sample, in micrograms.

We cultured *E.coli* nlp1 and *E.coli* tolR under identical conditions and isolated OMVs from them. OMVs can be detected indirectly by probing for the presence of outer membrane proteins that are present in most gram negative bacteria. The most common protein used for this purpose is Outer Membrane Protein A (OmpA) [19]. OmpA is a 37kDa constitutively expressed protein and is a protein marker for OMVs. To reliably use OmpA as a marker for OMVs, we verified that OmpA was present in all strains we utilised (Fig 3A). We also confirmed the presence of OmpA in the OMV fraction isolated from *E.coli* nlp1 and *E.coli* tolR (Fig 3B).

To visually confirm the presence of OMVs, we first imaged native OMVs isolated from *E. coli* tolR using a 120kV transmission electron microscope (Fig 3C). The images indicated the presence of heterogeneous spherical structures, 100–200 nm in diameter, consistent with the reported size range of OMVs. To better visualise the morphology of these structures, OMV sample was imaged by cryo-TEM, where we observed spherical structures with lipid bilayers,m confirming the presence of OMVs (Fig 3D).

Next, we measured the size distribution of OMVs isolated from E .coli nlp1 and *E. coli* tolR using dynamic light scattering (DLS). We found a strong correspondence between the two size distributions. Finally, we compared the yield of OMVs from the two strains (Fig 3E). The concentration of OMVs in a solution can be indirectly quantified using protein concentration as a proxy measure [19]. Protein quantification was performed using a Bradford Assay. A standard curve was constructed using Bovine Serum Albumin (BSA), and the regression line was used to compute protein concentrations of OMV samples. When subjected to the same culture conditions and isolation procedure, *E. coli* nlp1 yielded a higher amount of OMVs (Fig 3F). This may be due to intrinsic differences in the physiology of the two strains or due to differences in cell numbers. Therefore, we chose *E. coli* nlp1 for the remainder of the project.

Isolation of Engineered OMVs

We obtained gene fragments coding for the affibody proteins (ClyA-V5-Affi) and THP protein (ClyA-3XFLAG-THP). The parts were flanked by EcoN1 and BamH1 restriction sites which were used to ligate them into the plasmid pGEX-4T1. We successfully digested and ligated these parts into the backbone to produce pGEX-4T1 ClyA-V5-Affi and pGEX-4T1 ClyA-3XFLAG-THP (Fig 4A, 4B). We transformed these plasmids in *E.coli* DH5a and confirmed our clones by colony

PCR, restriction digestion and Sanger sequencing (Fig 4C, 4D, 4E).

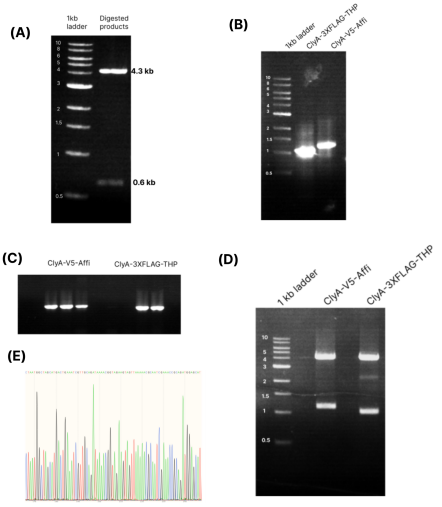

Figure 4. (A) Agarose gel image of the pGEX-4T1 backbone digested with EcoN1 and BamH1. (B) PCR amplification of gBlocks dsDNA gene fragments of ClyA-3X-FLAG (1049 bp) and ClyA-V5-Affi (1217 bp). (C) Agarose gel images of colony PCR to identify the positive clones. (D) Restriction digestion using the EcoN1 and BamH1 restriction sites released inserts corresponding to their expected sizes. (E) Representative chromatogram of Sanger sequencing of the sample ClyA-V5-Affi and ClyA-3XFLAG-THP. For ClyA-V5-Affi, three sequencing reactions were carried: two on the top strand and one on the bottom strand. For ClyA-3X-FLAG, two sequencing reactions were carried: one on the top strand and one on the bottom strand. On average, 300-400 bp of reads were obtained per reaction.

Following successful cloning, we transformed *E. coli* nlp1 to produce two populations: one containing pGEX-4T1 ClyA-V5-Affi and the other containing pGEX-4T1 ClyA-3XFLAG-THP, to produce Affi-OMVs and THP-OMVs respectively. Prior to isolating OMVs, we tested the expression of the proteins. We verified that full length ClyA-V5-Affii and ClyA-3XFLAG-THP were being produced, corresponding to the appropriate band sizes (Fig 5A).

Affi-OMVs containing ClyA-V5-Affi and THP-OMVs containing ClyA-3XFLAG-THP were isolated. We investigated the localisation of these proteins to the OMV fraction by Western blot. In both cases, we noted bands corresponding to the expected protein sizes (Fig 5B, 5C).

Western blots indicate that the recombinant proteins are present in the OMV fraction but do not provide information about the orientation of the protein. For Affi-OMVs and THP-OMVs to be internalised, it is important for the affibody and THP respectively to be present on the external surface of the OMV, and not in the lumen. A proteinase K test was carried out for Affi-OMVs to investigate this. Proteinase K is a non-specific protease. If the affibody and the tag are exposed on the outer surface, we expect them to be degraded or truncated following proteinase K treatment. If the affibody and tag are in the interior of the OMV, they should be protected from Proteinase K by the membrane, and should be intact. If OMVs are lysed with SDS prior to proteinase K treatment, then regardless of the orientation, we expect protein degradation. Our positive control (SDS +, Proteinase K +) did not work and we did not obtain any conclusive results from this experiment (Fig 5D).

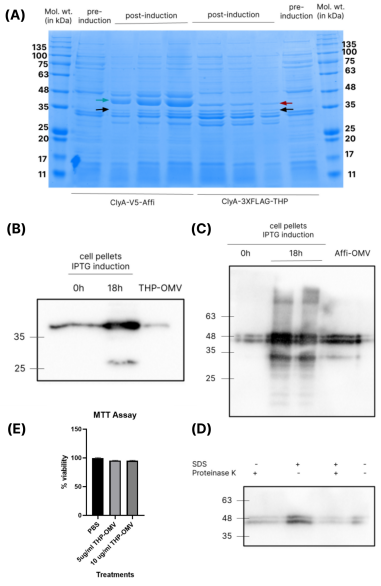

Figure 5. (A) SDS PAGE gel image indicating expression of ClyA-V5-Affi (green arrow) and ClyA-3XFLAG-THP (red arrow) in the bacterial cells following IPTG induction. Lower molecular weight bands (black) are also visible in both cases post-induction. (B) Anti-FLAG Western blot of bacterial cells (before and after induction) and THP-OMV fraction. A band corresponding to ClyA-3XFLAG-THP at 37kDa is visible in all lanes, suggesting the production and localization of ClyA-3XFLAG-THP to the OMV fraction. (C) Anti-V5 Western blot of bacterial cells (before and after induction) and Affi-OMV fraction. A band at the appropriate corresponding to ClyA-V5-Affi at 45kDa is visible in all lanes, suggesting the production and localization of ClyA-V5-Affi to the OMV fraction. Significant background signal was also obtained. Low levels of expression occurring prior to induction were noted in both (B) and (C). (D) Results of the Proteinase K test performed on Affi-OMVs. OMVs were incubated with or without SDS and with or without Proteinase K, as indicated. The entire volume of the reaction was analysed by Western blot against the V5 tag. (E) Cytotoxicity of THP-OMVs as measured using the MTT assay with SK-BR-3 cell cultures. The mean percentage viability is reported as the viability of THP-treated SK-BR-3 cells normalised to the mean viability following PBS treatment. Viability is reported as mean ± standard error of mean of three biological replicates. Concentrations of THP-OMVs indicated are working concentrations.

Investigating safety of engineered OMVs

The MTT assay is a colorimetric assay for assessing cell metabolic activity, and can be used to measure cell viability. In this case, we aimed to measure cell viability following treatments of different concentrations of THP-OMVs expressing ClyA-3XFLAG-THP, as compared to a control treatment of 1X PBS. SK-BR-3 cells were utilised for this assay. The mean percent-

age viability is reported as the viability of THP-OMV treated SK-BR-3 cells normalised to the mean viability following PBS treatment (Fig 5E).

Testing Internalisation of Engineered OMVs in Mammalian Cell Lines

We aimed to test the selective internalisation of Affi-OMVs and THP-OMVs into a cell line overexpressing both target markers, HER2 and CX3CR1, compared to a negative control cell line with low expression of the markers. The test cell line was SK-BR-3, and the negative control was HEK 293T. They were chosen due to relative differences in the expression of HER2 and CX3CR1 [21].

We designed different treatments to study internalisation (Table 1). Internalisation was detected with immunocytochemistry (ICC) and Western blot. Total protein content in the OMVs was used as a proxy measure for OMV quantity. We incubated SK-BR-3 and HEK 293T cells with OMVs for 4-5h at 37°C. After washing, fixation and staining, we visualised the localization of OMVs by confocal microscopy (Fig 6A. 6B, 6C, 7A, 7B).

Table 1. OMVs treatment plan

Treatment	SK-BR-3 (1)	SK-BR-3 (2)	SK-BR-3 (3)	SK-BR-3 (4)	HEK 293T (5)
Type of OMVs used for treatment	Native OMVs	Affi-OMVs	THP-OMVs	Affi-OMVs +THP-OMVs	Affi-OMVs +THP-OMVs
OMV quantity	5 μg	5 μg	5 μg	5 μg+5μg	5 μg+5μg
Protein probed	OmpA	V5 tag	3XFLAG tag	V5, 3XFLAG	V5, 3XFLAG

We performed a blinded image analysis of the internalisation studies. From this preliminary data we arrived at the following conclusions:

1. We did not observe any significant association of native OMVs with SK-BR-3 cells in most fields during imaging.
2. Upon treating SK-BR-3 with Affi-OMVs, we observed interaction with the cell membrane. This is possibly explained by the binding of the affibody present on Affi-OMvs to HER2 present on the cell surface.
3. A similar result was observed upon treating SK-BR-3 with THP-OMVs, with signal being detected interior to the cell boundary. We hypothesise this is due to receptor mediated internalisation following binding of the THP to CX3CR1 present on the cell membrane.
4. When Affi-OMVs and THP-OMVs are co-incubated with SK-BR-3 cells, signal from both is detected, suggesting the internalisation of both types of OMVs.
5. When Affi-OMVs and THP-OMVs are co-incubated with HEK 293T cells, we observed both types of OMVs to be present as aggregates in the extracellular media.

We found encouraging evidence that suggests that Affi-OMVs and THP-OMVs selectively internalise in cells overexpressing their target markers HER2 and CX3CR1 respectively.

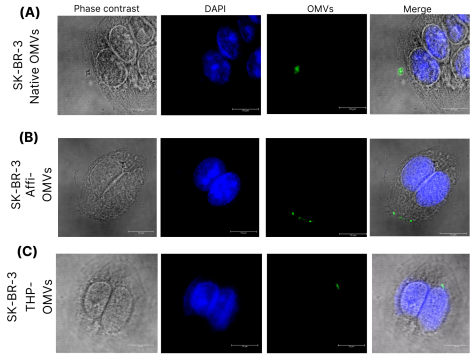

Figure 6. (A) OMVs (green) are visualised by rabbit anti-OmpA antibodies. Signal was detected from the extracellular region. (B) ffi-OMVs (green) expressing ClyA-V5-Affi are visualised by rabbit anti-V5 antibodies. Signal was detected at the periphery of cells, indicating cell binding and possibly internalisation. (C) THP-OMVs (green) expressing ClyA-3XFLAG-THP are visualised by anti-FLAG antibodies. Signal is detected from the cytoplasm of the cell, indicating internalisation.

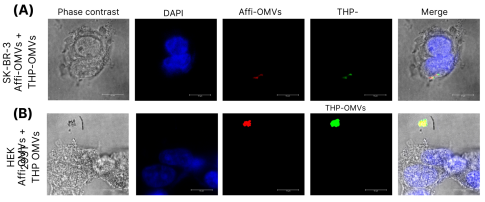

Figure 7. Affi-OMVs (red) expressing ClyA-V5-Affi are visualised by anti-V5 antibodies and anti-rabbit Alexa Fluor 633. THP-OMVs (green) expressing ClyA-3XFLAG-THP are visualised by anti-FLAG antibodies and anti-mouse Alexa Fluor 488. (A) Signal from both OMVs was detected from the cytoplasm, suggesting internalisation. (B) Signal was detected from the extracellular media.

Discussion

To summarise, we have developed a functional, flexible, and adaptable dual OMV system, and provided a preliminary proof of principle. We successfully isolated native OMVs from a hypervesiculating strain of *E. coli* and verified the presence of OMVs in the isolated fraction. We produced both types of engineered OMVs and confirmed the localization of the affinity proteins to the OMV fraction. We also tested the internalisation of the affi-OMVs and THP-OMVs in the cell lines SK-BR-3 and HEK 293T, and found that the engineered OMVs internalised in the breast cancer cell line but did not internalise in the non-cancerous cell line.

There are some limitations with this study. The internalisation experiments were not carried in replicates, limiting our ability to generalise these results. While HEK 293T is not a breast cancer cell line, it is not representative of a non-cancerous cell in the human body. We also observed aggregation of OMVs and possible non-specific signals during microscopy. We did not assess the safety of affi-OMVs, but we believe the results for the THP-OMVs can be mapped to the affi-OMVs. FInally, for safety reasons we did not perform experiments with the cytotoxic 5 FU/cytosine deaminase, and hence we did not obtain a full picture of the functioning of Duonco.

Future Directions

In this section we will broadly outline the experiments needed to further assess the efficacy of our drug delivery system. For the purpose of this project we utilised SK-BR-3 to study internalisation, and we are interested in replicating these results in other breast cancer cell lines such as MCF-10A and MCF-7. The fate of OMVs upon internalisation and subsequent release of cargo is not well understood. The former can be studied by loading OMVs with fluorescent molecules and tracking them inside the cell via live cell imaging and the latter can be studied by a split GFP assay. Though K-12 strains have reduced LPS levels, we would also like to measure the level of LPS associated with our isolated OMVs using the LAL assay. Most importantly, we would like to load the OMVs with the prodrug/enzyme cargo to see if sufficient cytotoxicity in cancer cells can be achieved.

For future development of the system, testing in animal models required to monitor off-target effects, immune response, and dosage. Clinical trials would follow where we will investigate additional questions such as maximum tolerated doses, pharmacokinetics, and dynamics to determine the system's safety. Trials would also investigate additional therapy regimens, target populations, drug-drug interactions, and dose-response to find the optimum possible usage of the system.

Duonco was originally developed for HER2+ breast cancer cases, but we intend to expand it to other forms of cancer by modifying the targeting affinity proteins on the surface of the OMVs. With the expanded use of genetic sequencing, patients' unique gene expression profiles can be leveraged to highly personalise drug delivery systems.

Lastly, we want to investigate several approaches for mass-producing these tailored OMVs at a low cost. Despite the fact that our method ensures little contamination and high-quality OMVs, the net yield remains a challenge. This can be avoided by building a bioreactor, which is a more secure alternative to single-batch cultures. It is possible to maintain a continuous culture with a lower risk of contamination by limiting the number of times humans are required to intervene. Our proposed bioreactor would be able to handle large volumes of bacterial cultures and would incorporate a centrifuge and allow us to establish a continuous batch culture followed by high throughput purification by density gradient centrifugation and gel filtration to achieve a homogeneous yield of OMVs.

Materials and Methods

Bacterial Stains and Culturing Conditions

E. coli K12 tolA::Kan, tolR::Kan, nlp1::Kan, degP::Kan were obtained from the Keio collection and cultured in standard LB broth supplemented with with 25 microgram/ml kanamycin at 37°C, 180rpm. *E. coli* DH5alpha and *E. coli* Mach1 cells were used for transformation and plasmid isolation, were sourced from LICB and Host-Pathogen Interaction Lab, IISER TVM respectively. The cells were made competent via the CaCl2 method. Following transformation, bacterial cells were cultured in standard LB broth supplemented with 100 microgram/ml ampicillin at 37°C, 180rpm.

Detailed protocols for media preparation, bacterial cultures, growth curve construction and competent cell preparation can be found in the supplementary material.

Cloning

dsDNA gBlock fragments coding for ClyA-V5-Affi and ClyA-3XFLAG-THP were obtained from Integrated DNA Technologies, with an EcoN1 site upstream and BamH1 site downstream. PCR amplification of the gene fragments with a high-fidelity polymerase was carried out, followed by restriction digestion by EcoN1 and BamH1. The plasmid backbone pGEX-4T1 was provided by Dr. Vipul Gujrati, TUM Germany. The double digested backbone with cohesive ends was ligated with the digested inserts by the T4 DNA ligase and the mixture was transformed into *E. coli* DH5a. Positive transformants were screened by colony PCR, and positive clones were verified by Sanger sequencing and restriction digestion. Plasmid was isolated, and used to transform *E. coli* nlp1.

Detailed protocols for PCR, restriction digestion, PCR cleanup, gel extraction, ligation, transformation, colony PCR, Sanger sequencing and plasmid isolation can be found in the supplementary material.

OMV Isolation

An overnight primary bacterial culture was standardised to OD 600=1 and diluted 1/100 into a secondary culture of volume 400 ml. If native OMVs were to be isolated, the secondary culture was grown for 18 hrs 37°C. If engineered OMVs were to be isolated, the culture was grown to mid-log (OD600 = 0.4-0.6) at 37°C and induced with 1mM IPTG, and grown for 18h. To obtain a cell-free supernatant, the culture was centrifuged at 5000 g for 30 minutes (Sorvall Lynx 5000 High Speed Centrifuge). The supernatant was membrane filtered through a 0.22um filter. The filtrate was centrifuged at 20,000 g for 3h 4°C (Sorvall Lynx 5000 High Speed Centrifuge). A final round of centrifugation was carried out at 28,000 g for

4h at 4°C (Beckman XPN Optima Ultracentrifuge). The supernatant was discarded and the pellet containing OMVs was resuspended in 100 microliter of PBS. The OMVs that were isolated were then stored at -20°C.

Detailed protocols can be found in the supplementary material.

Dynamic Light Scattering (DLS)

All experiments were performed in a Malvern Zetasizer Nano ZS. 40 uL samples of OMVs suspended in 1XPBS suspensions were added to washed disposable cuvettes (ZEN0040). Samples were diluted by adding 500 uL of 1X PBS. Measurements were taken at standard angles at 25°C with an equilibration time of 60 seconds.

Detailed settings and specifications can be found in the supplementary material.

Transmission Electron Microscopy and Cryogenic Transmission Electron Microscopy

Visualisation of isolated OMVs was performed using transmission electron microscope (Fei-Tecnai G2 Spirit BioTWIN-120kV). All samples had a dilution ratio of 1:15 and 5-6 microlitre of the samples were dropcasted on carbon-coated copper grid (400 mesh) and left overnight (>12 hours). The samples were stained using 1 percent or 4 percent phosphotungstic acid solution and left overnight again (>12 hours). For Cryogenic transmission electron microscopy (cryo-TEM, OMVs samples were dropcasted on a copper grid before imaging. TEM was carried out at IISER Thiruvananthapuram, and cryo-TEM was carried out at IISc, Bengaluru.

Western Blotting

The protein concentration was initially estimated using a Bradford Assay (following the protocol of Bio-Rad). The OMVs were lysed using a lamelli buffer. A 10 percent gel resolving was used for the SDS PAGE and following electrophoresis the proteins were transferred onto a PVDF membrane at 90V for 3h. The membrane was blocked overnight in 5 percent non fat milk in TBS. This was followed by a 3 hour incubation with the primary antibody and 1 hour incubation with the secondary antibody. The membrane was developed and visualised using standard protocols (BIO RAD chemidoc XRS+).

Detailed protocols for the Bradford assay, SDS PAGE, Coomassie staining, Western transfer, Proteinase K assay and the list of antibodies used, with their dilutions can be found in the supplementary material.

Mammalian Cell Culture and MTT Assay

The cells were cultured at 37°C, 5 percent CO2 in 35mm dishes. SK-BR-3 was cultures in McCoy's Media and HEK 293T was cultured in DMEM. SK-BR-3 cells were used for the MTT assay. After counting cells with a hemocytometer, 5000 SK-BR-3 cells were seeded in 200microlitre of McCoy's media in wells in a 96 well plate. After incubation for 36h, the media was aspirated and replaced with a mixture of OMVs and media and incubated for 5h. Each treatment was carried in triplicate. 100v microlitre of the MTT reagent was added to each well, and cells were incubated for 24h. The supernatant was aspirated and 100 microlitre of DMSO was added, and the plate was incubated for 10 min. Absorbance was measured at 565 nm (Tecan Infinite M200PRO).

Cell Internationalisation Experiments

Refer to the table 1 for the experimental setup.

Cells were seeded in 6 well plates with confluency of 60-70 percent in McCoy's media and incubated for 24h. The media was aspirated and replaced with fresh serum-free media (SFM) + 1X PenStrep. The 6 well plates each were treated with OMVs as in Table 1 for 5h. Following incubation, 1 ml of ice-cold methanol was added and incubated for 5 min. The coverslips were washed in PBS and placed into a humid staining chamber. PBSAT blocking buffer was added to each coverslip and incubated for 25 min. The blocking step was repeated and primary antibodies were added to the respective coverslips and incubated for 1 hour. After washing with 1 ml 1X PBS and a 2 min incubation with 20 microlitre DAPI per coverslip, the cells were given a 1 ml 1X PBS wash. Finally, the coverslips were incubated for 10h with ProLong Gold Antifade reagent and imaged under confocal microscopy.

Complete protocols are available in the supplementary material.

Biosafety

The design of Duonco is such that it aims to be a safer alternative to existing chemotherapies for breast cancer. Like any drug delivery system, it can potentially be used to deliver a harmful payload to a human or an animal subject. We do not believe that our project has an increased risk for dual use above and beyond what is already available in literature. OMVs are non-replicating, which reduces the risk of unwanted spread. Isolating OMVs requires sophisticated equipment such as ultracentrifuges, which restricts its usage to research institutions. Given that the prodrug-enzyme is cytotoxic mammalian cells and human, we avoided carrying out experiments with it. The gene cytolysin A (which forms the N terminus of the recombinant affinity proteins) is known to be toxic to mammalian cells. Hence we consulted Dr. Rahul Roy (IISc Bengaluru), an expert on ClyA, and created a mutant version ClyA171F which is safer. We also experimentally quantified the safety of the recombinant affinity protein and engineered OMVs via an MTT assay and did not find much cytotoxicity of these components. Our project has been approved by the IBSC (Institutional Biosafety Committee). Our research and work development applications were considered and noted by the Review Committee on Genetic Manipulation (RCGM under

DBT) in its 228th meeting held on March 17, 2022. Our PhD mentors and advisors guide us at each stage of the project, and the institute safety officer inspects and approves all aspects of our proposal.

Contributions

Ananya Aravind designed media, performed education outreach and human practices. Devashish Kalmegh contributed media, performed outreach, filmed and edited the presentation video. Harshini Sivanganam contributed to experimental design, carried out cloning western blotting, performed literature survey and wrote this report. Gopal K. contributed media, filmed and edited the presentation video. Ira Zibbu contributed to experimental design, carried out cloning western blotting, performed literature survey, analysed and plotted results and wrote this report, Jyothi S. contributed to educational outreach and fundraising. Kapavarapu Pratham performed literature survey, raised funding, and contributed to educational outreach and human practices. Kavya Sunil planned and carried out stakeholder interactions, and performed outreach. Merina Tony planned and carried out stakeholder interactions, and assessed project safety. Nikhil Nawaz performed mathematical modelling. Parth Ankam performed cloning, and conducted literature review. Pranav Thapron contributed to experimental design, carried out OMV isolation and mammalian cell culture, conducted literature survey, assessed project safety and wrote this report. Riya Shende contributed to experimental design, carried out OMV isolation and mammalian cell culture, conducted literature survey, and wrote this report. Siddharth Kurne conducted literature survey, contributed to experimental design, and performed the MTT assay. Sneha P. R. managed the team and project, conducted literature review, and contributed to outreach, human practices and funding.

We would like to thank our PIs, Prof. S Murty Srinivasula and Dr. Sandhya Ganesan, School of Biology, IISER Thiruvananthapuram, and Prof. Dipshikha Chakravortty, IISc Bengaluru. We thank our PhD mentors T. M. Tejas, Delvin Pauly, Krishanu Dey Das, and Abhishek Raghunathan. We appreciate the help provided by Dr. Somnath Dutta, IISc, for cryo-TEM and Dr. Vipul Gujrati for sending us the plasmids. We wish to acknowledge the technical assistants from School of Biology, IISER Thiruvananthapuram. We thank our sponsors.

References

1. Di Nardo, P. et al. Chemotherapy in patients with early breast cancer: clinical overview and management of long-term side effects. Expert Opinion on Drug Safety 21, 1341–1355 (2022).
2. Ferlay, J. et al. Estimating the global cancer incidence and mortality in 2018: GLOBOCAN sources and methods. Int J Cancer 144, 1941–1953 (2019).
3. Rajpal, S., Kumar, A. Joe, W. Economic burden of cancer in India: Evidence from cross-sectional nationally representative household survey, 2014. PLoS ONE 13, e0193320 (2018).
4. Zhu, C. et al. Safety and efficacy evaluation of pertuzumab in patients with solid tumors. Medicine (Baltimore) 96, e6870 (2017). .
5. Yu, S. et al. Development and clinical application of anti-HER2 monoclonal and bispecific antibodies for cancer treatment. Exp Hematol Oncol 6, 31 (2017).
6. Eliyatkin, N., Yalcin, E., Zengel, B., Aktaş, S. Vardar, E. Molecular Classification of Breast Carcinoma: From Traditional, Old-Fashioned Way to A New Age, and A New Way. J Breasth Health 11, 59–66 (2015).
7. Patel, A., Unni, N. Peng, Y. The Changing Paradigm for the Treatment of HER2-Positive Breast Cancer. Cancers (Basel) 12, 2081 (2020).
8. Shen, F. et al. Novel Small-Molecule CX3CR1 Antagonist Impairs Metastatic Seeding and Colonization of Breast Cancer Cells. Mol Cancer Res 14, 518–527 (2016).
9. Schwechheimer, C. Kuehn, M. J. Outer-membrane vesicles from Gram-negative bacteria: biogenesis and functions. Nat Rev Microbiol 13, 605–619 (2015).
10. Kuerban, K. et al. Doxorubicin-loaded bacterial outer-membrane vesicles exert enhanced anti-tumor efficacy in non-small-cell lung cancer. Acta Pharm Sin B 10, 1534–1548 (2020).
11. Kim, O. Y. et al. Bacterial outer membrane vesicles suppress tumor by interferon--mediated antitumor response. Nat Commun 8, 626 (2017).
12. Eigenbrot, C., Ultsch, M., Dubnovitsky, A., Abrahmsén, L. Härd, T. Structural basis for high-affinity HER2 receptor binding by an engineered protein. Proc. Natl. Acad. Sci. U.S.A. 107, 15039–15044 (2010).
13. Pereira, A. C. et al. Selection of a new peptide homing SK-BR-3 breast cancer cells. Chem Biol Drug Des 97, 893–903 (2021).
14. Kondo, E., Iioka, H. Saito, K. Tumor-homing peptide and its utility for advanced cancer medicine. Cancer Sci 112, 2118–2125 (2021).
15. Gujrati, V. et al. Bioengineered Bacterial Outer Membrane Vesicles as Cell-Specific Drug-Delivery Vehicles for Cancer Therapy. ACS Nano 8, 1525–1537 (2014).
16. Malekshah, O. M., Chen, X., Nomani, A., Sarkar, S. Hatefi, A. Enzyme/Prodrug Systems for Cancer Gene Therapy. Curr Pharmacol Rep 2, 299–308 (2016).
17. Longley, D. B., Harkin, D. P. Johnston, P. G. 5-Fluorouracil: mechanisms of action and clinical strategies. Nat Rev Cancer 3, 330–338 (2003).
18. Shrivastava, R., Jiang, X. Chng, S.-S. Outer membrane lipid homeostasis via retrograde phospholipid transport in *Escherichia coli*: A physiological function for the Tol-Pal complex. Molecular Microbiology 106, 395–408 (2017).
19. Reimer, S. L. et al. Comparative Analysis of Outer Membrane Vesicle Isolation Methods With an Escherichia coli tolA Mutant Reveals a Hypervesiculating Phenotype With Outer-Inner Membrane Vesicle Content. Front. Microbiol. 12, 628801 (2021).
20. Schwechheimer, C. Kuehn, M. J. Synthetic Effect between

Envelope Stress and Lack of Outer Membrane Vesicle Production in Escherichia coli. Journal of Bacteriology 195, 4161–4173 (2013).
21. Sjöstedt, E. et al. An atlas of the protein-coding genes in the human, pig, and mouse brain. Science 367, (2020).